Proceedings of the 11th World Congress in Mechanism and Machine Science
August 18–21, 2003, Tianjin, China
China Machinery Press, edited by Tian Huang

Sensor Requirements for Tyre Force Estimation; Applications to Off-Highway Mining Trucks

P.M. Siegrist and P. R. McAree
CRC for Mining Technology and Equipment (CMTE) and Department of Mechanical Engineering, The University of Queensland, St. Lucia 4072, AUSTRALIA
e-mail: {p.siegrist,p.mcaree}@uq.edu.au,

Abstract: The tyre force components acting at the tyre road interface of an off-highway mining truck are estimated using an Extended Kalman filter (EKF). The EKF combines an 11 dof dynamic model of the truck with inertial sensor measurements from the truck sprung and un-sprung bodies. The tyre force estimates have been compared with the actual tyre forces from an advanced virtual truck model.

Keywords: Estimation theory, mining, haul trucks, tyre forces.

1 Introduction

This paper describes a method for estimating tyre forces on off-highway mining dump trucks. We deal specifically with the sensor requirements.

Off-highway mining dump trucks are large, rigid frame trucks used in open pit mining operations to transport oar and waste material from the mined surface to the crusher and dump areas, see Martin *et al.* (1981). These trucks have typical payloads greater than 150 tonnes. The combination of high payloads, surface irregularities, and driver actions generate dynamic forces at the tyre/road interface that are, typically, two to three times static loads (Prem 1998). High forces in conjunction with relative slip between the road and the tyre lead to high rates of tyre wear.

This work is part of a project to develop an on-line truck tyre wear monitor. The monitor aims to detect regions of high tyre wear by estimating the forces and slip at the tyre/road surface. The first phase of the project is to estimate the tyre forces.

This paper describes the application of the extended Kalman filter to estimate tyre forces by combining inertial sensor measurements from the truck's body with a model of the truck dynamics in the presence of model and measurement uncertainty. The estimates require no knowledge of tyre or suspension parameters. The approach builds on that described in Ray (1995) and Ray (1997) by including the estimation of vertical components of tyre forces and overcoming the need for difficult-to-make velocity measurements.

Figure 1. A large off-highway mining truck

2 The Extended Kalman Filter

The continuous-discrete Extended Kalman filter (EKF) estimates the state of continuous, non-linear, stochastic, dynamic systems with discrete measurements described by

$$\dot{\mathbf{x}} = \mathbf{f}\left(\mathbf{x},\mathbf{u},t\right) + \mathbf{w}, \quad \mathbf{w} \sim \mathrm{N}\left(\mathbf{0},\mathbf{Q}\right) \tag{2.1}$$

$$\mathbf{z}_k = \mathbf{h}\left(\mathbf{x},\mathbf{u},k\right) + \mathbf{v}, \quad \mathbf{v} \sim \mathrm{N}\left(\mathbf{0},\mathbf{R}\right) \tag{2.2}$$

where $\mathbf{f}\left(\mathbf{x},\mathbf{u},t\right)$ and $\mathbf{h}\left(\mathbf{x},\mathbf{u},k\right)$ are non-linear functions of the state, $\mathbf{x}$, the input vector, $\mathbf{u}$ and time. Note Eqn. (2.1) continuous; Eqn. (2.2) is discrete. The variables $\mathbf{w}$ and $\mathbf{v}$, are assumed to be generated by zero mean, Gaussian processes with covariances $\mathbf{Q}$ and $\mathbf{R}$ respectively; $\mathbf{w}$ is commonly termed the process noise and $\mathbf{v}$ the measurement noise.

The computational scheme of the EKF involves five steps Gelb (1974):

1. State estimate propagation

$$\dot{\mathbf{x}} = \mathbf{f}\left(\mathbf{x},\mathbf{u},t\right) \tag{2.3}$$

2. Error covariance propagation

$$\dot{\mathbf{P}} = \Delta\mathbf{f}\mathbf{P} + \mathbf{P}\Delta\mathbf{f}^{\mathrm{T}} + \mathbf{Q} \tag{2.4}$$

3. Calculation of the Kalman gain

$$\mathbf{K}_k = \mathbf{P}_k^{-}\Delta\mathbf{h}_k{}^{T}\left(\Delta\mathbf{h}_k\mathbf{P}_k^{-}\Delta\mathbf{h}_k{}^{T} + \mathbf{R}_k\right)^{-1} \tag{2.5}$$

4. State estimate update

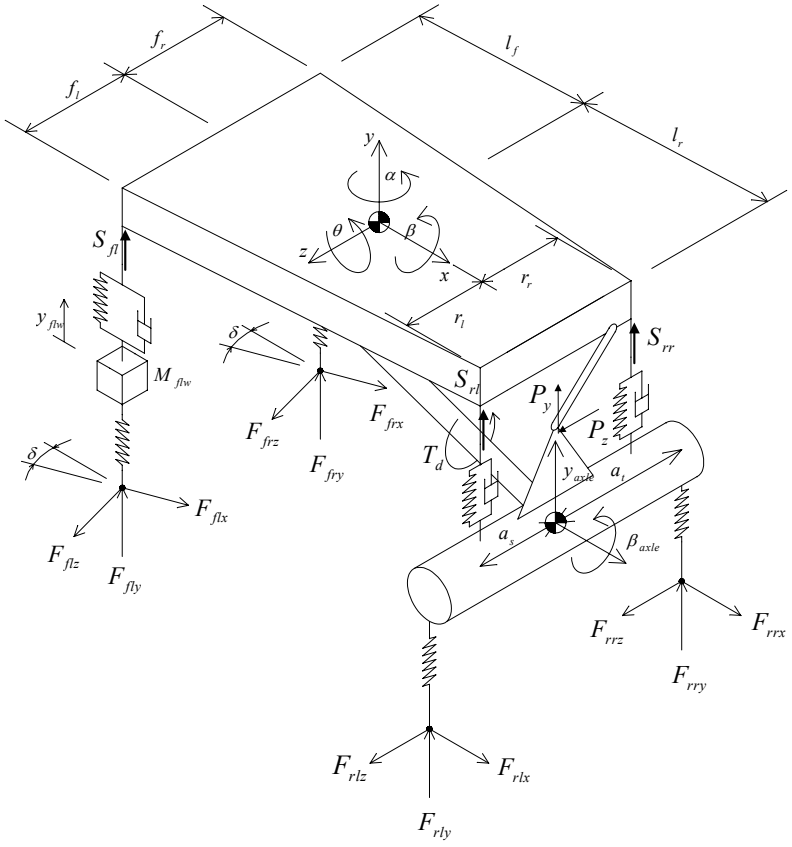

Figure 2. The estimation model

$$\hat{\mathbf{x}}_k^+ = \hat{\mathbf{x}}_k^- + \mathbf{K}_k\left(\mathbf{z}_k - \mathbf{h}_k\left(\hat{\mathbf{x}}_k^-, \mathbf{u}_k^-, k\right)\right) \qquad (2.6)$$

5. Error covariance update

$$\mathbf{P}_k^+ = \left(\mathbf{I} - \mathbf{K}_k \Delta\mathbf{h}_k\right)\mathbf{P}_k^- \qquad (2.7)$$

The superscripts - and + indicate before and after a measurement has been made and the terms $\Delta\mathbf{f}$ and $\Delta\mathbf{h}$ are the Jacobians

$$\Delta\mathbf{f} = \left.\frac{\partial\mathbf{f}\left(\mathbf{x},\mathbf{u},t\right)}{\partial\mathbf{x}}\right|_{\mathbf{x}=\hat{\mathbf{x}}} \qquad (2.8)$$

$$\Delta\mathbf{h}_k = \left.\frac{\partial\mathbf{h}\left(\mathbf{x}_k,\mathbf{u}_k,k\right)}{\partial\mathbf{x}_k}\right|_{\mathbf{x}_k=\hat{\mathbf{x}}_k} \qquad (2.9)$$

The Kalman filter produces an optimal updated state estimate, $\hat{\mathbf{x}}_k^+$, that minimises the state error covariance, $\mathbf{P}$.

To ensure the state estimates are convergent, two conditions must be met, see Rief *et al* (1999):
(i) The system must be observable. This condition ensures that the covariance of the state estimation error will always decrease when measurements are made (new information is added to the system) .
(ii) The system must be controllable. This condition ensures that the Kalman filter gain matrix influences all the states.

The system we are dealing with here is non-linear making it difficult to establish these conditions in a strict technical sense. We use a relaxed condition, requiring only local controllability and observability, justified by the underlying dynamic equations being smooth (free of singularities) in the range of expected operation. Conditions for observability and controllability are realized when the observability and controllability Gramians of the linearized systems about an operating point are full rank.

3 The estimation model

The estimation model is based on a simplified 3D truck shown in Figure 2. The sprung mass is assumed a rigid body. The front suspension is independent and the rear uses a suspended rigid axle with a panhard rod providing the lateral location. The torque is delivered to the rear axle via a drive shaft and is then distributed to the rear wheels through a differential located inside the axle. The front wheels are steerable by an angle, δ. Braking is applied through a braking torques, B, at each wheel. The subscripts, fl, fr, rl and rr indicate the front left, front right, rear left and rear right wheels respectively. The tyre forces to be estimated are the lateral, F_x, the vertical, F_y, and the longitudinal, F_z, at each tyre. Gravity is given by g.

The rigid-body dynamics are the defined by Eqns. (3.1), (3.2) and (3.3). These are the translational longitudinal and lateral modes and rotational yaw mode respectively. The truck is assumed to yaw about an axis perpendicular to the road plane passing through

the truck's centre of gravity. The total mass of the truck is given by M_t, and the total yaw inertia is I_y. The equations are defined with respect to an axis system located at the truck's center of mass.

$$\begin{aligned} I_y\alpha = {} & F_{rlx}r_l - F_{rrx}r_r - \left(F_{rlz} + F_{rrz}\right)l_r \\ & + \cos\delta\left(F_{flx}f_l + F_{flz}l_f - F_{frx}f_r + F_{frz}l_f\right) \\ & - \sin\delta\left(F_{flx}l_f - F_{flz}f_r + F_{frx}l_f + F_{frz}f_r\right) \end{aligned} \quad (3.3)$$

The sprung mass dynamics are the bounce, pitch, and roll of the truck body described by Eqns. (3.4), (3.5) and (3.6). The mass of the truck body is M_b and the body inertias I_{bx} and I_{bz}. The forces in the suspension struts are given by S. The perpendicular distance from the tyre road contact to center of mass is given by h.

$$M_b\ddot{y} = S_{fl} + S_{fr} + S_{rl} + S_{rr} - M_b g \quad (3.4)$$

$$\begin{aligned} I_{bx}\ddot{\beta} = {} & F_{rrz}h_{rr} + F_{rlz}h_{rl} - F_{flx}h_{fl}\sin\delta \\ & - F_{frx}h_{fr}\sin\delta + F_{flz}h_{fl}\cos\delta \\ & + F_{frz}h_{fr}\cos\delta \\ & + S_{fr}f_r + S_{rr}r_r - S_{fl}f_l - S_{rl}r_l \end{aligned} \quad (3.5)$$

$$\begin{aligned} I_{bz}\ddot{\theta} = {} & F_{rrx}h_{rr} + F_{rlx}h_{rl} + F_{flz}h_{fl}\sin\delta \\ & + F_{frz}h_{fr}\sin\delta + F_{flx}h_{fl}\cos\delta \\ & + F_{frx}h_{fr}\cos\delta \\ & + l_r\left(S_{rl} + S_{rr}\right) - l_f\left(S_{fl} + S_{fr}\right) \end{aligned} \quad (3.6)$$

The unsprung mass dynamics are defined in Eqns. (3.7) to (3.10). These are the front wheel and rear axle bounce modes and the rear axle pitch mode. The front suspension of the truck is independent with the front wheels only able to translate normal to the road plane. The rear axle can both pitch and bounce. Pitching is assumed to occur about the axle's center of mass.

$$M_{flw}\ddot{y}_{flw} = F_{fly} - S_{fl} - M_{flw}g \quad (3.7)$$

$$M_{frw}\ddot{y}_{rlw} = F_{fry} - S_{fr} - M_{frw}g \quad (3.8)$$

$$M_{axle}\ddot{y}_{axle} = F_{rly} + F_{rry} - S_{rl} - S_{rr} - P_y - M_{axle}g \quad (3.9)$$

$$\begin{aligned} I_{axle}\ddot{\beta}_{axle} = {} & F_{rry}a_t - F_{rly}a_t + S_{rl}a_s - S_{rr}a_s \\ & + P_z a_p + T_d - F_{rlz}r_{rlw} - F_{rrw}r_{rrw} \end{aligned} \quad (3.10)$$

Each wheel's rotational dynamics are defined in Eqns. (3.11) to (3.14), where the I's are the rotational inertias of the wheels and the r's the rolling radii. The four wheels commonly found on the rear axle of an actual mining truck have been simplified into one wheel on each side of the axle. Rolling resistance is neglected.

$$\begin{aligned} M_t\ddot{x} = {} & F_{rrx} + F_{rlx} + \left(F_{flx} + F_{frx}\right)\cos\delta \\ & + \left(F_{frz} + F_{flz}\right)\sin\delta \end{aligned} \quad (3.1)$$

$$\begin{aligned} M_t\ddot{z} = {} & F_{rrz} + F_{rlz} + \left(F_{flz} + F_{frz}\right)\cos\delta \\ & - \left(F_{frx} + F_{flx}\right)\sin\delta \end{aligned} \quad (3.2)$$

$$I_{flw}\dot{\omega}_{flw} = F_{flx}r_{flw} + B_{fl} \quad (3.11)$$

$$I_{frw}\dot{\omega}_{frw} = F_{frx}r_{flw} + B_{fr} \quad (3.12)$$

$$I_{rlw}\dot{\omega}_{rlw} = F_{rlx}r_{rlw} + T_d + B_{rl} \quad (3.13)$$

$$I_{rrw}\dot{\omega}_{rrw} = F_{rrx}r_{rrw} + T_d + B_{rr} \quad (3.14)$$

Inspection of the 3D model's equations of motion reveal that there is insufficient information to individually observe each lateral tyre force. The additional information needed either includes relating the lateral acceleration of each tyre to the lateral forces via an effective tyre mass, or by relating the lateral displacement of the each tyre at the road contact to lateral force via the lateral tyre displacement stiffness. Neither of these options are feasible as they require measurements to be made directly from the truck's tyres. An observable system can only be obtained for one combined front lateral force and one combined rear lateral force.

Further inspection of the equations also reveals that, there is no benefit in including the sprung-body bounce, roll and pitch dynamics into the estimation model. Removal of these equations relives the need of knowing the roll and pitch axis heights.

In a state space model, forces are generally regarded as inputs. However, here the forces must be included as states such that they can be estimated. This is achieved by using an adaptation of state augmentation (Gelb, 1974) where the tyre forces are regarded as correlated noise inputs. The tyre force correlation is modelled in a shaping filter driven by a white noise process, Eqn (3.15), which is augmented to the state vector.

$$\begin{bmatrix} \dot{F} \\ \ddot{F} \end{bmatrix} = \begin{bmatrix} 0 & 1 \\ 0 & 0 \end{bmatrix}\begin{bmatrix} F \\ \dot{F} \end{bmatrix} + \begin{bmatrix} 0 \\ p \end{bmatrix} \quad (3.15)$$

The dynamic behaviour of the shaping filter is dependent on the magnitude of the driving noise, p. For large values of driving noise variance the forces will be fast to respond but will be sensitive to noise sources. For smaller driving noise variances there is less noise attenuation but response time is slower.

The state vector of the estimation model takes the form

$$\mathbf{x} = \begin{bmatrix} \alpha & \omega_{fl} & \omega_{fr} & \omega_{rl} & \omega_{rr} & \left[\mathbf{F}\right] \end{bmatrix}^T$$

where $\left[\mathbf{F}\right]$ is a vector containing the ten tyre forces and their derivatives.

The inputs, $\mathbf{u}$, to the system are the steering angle, braking and driving torque, the strut forces and the longitudinal and lateral forces transmitted to the rear axle through the panhard rod. The driving torque and strut forces can be taken from existing OEM on-board truck monitoring systems. The steering angle can be measured as a displacement on the steering rack or an angular displacement on the driver's steering wheel. Braking torque can be measured from the pressure in the hydraulic brake lines. The force transmitted through the panhard rod can be measured with a strain gauge. The strut and panhard rod forces are included as inputs rather than measurements to prevent the need for additional states in the state vector.

$$\mathbf{u} = \begin{bmatrix} \delta & T_d & B_{fl} & B_{fr} & B_{rl} & B_{rr} & S_{fl} & S_{fr} & S_{rl} & S_{rr} & P_y & P_z \end{bmatrix}^T$$

The measurement vector that insures all the states are observable includes the lateral and longitudinal accelerations, the yaw rate, the wheel speeds, the front wheel and rear axle vertical acceleration and the rear axle angular acceleration. The rear axle angular acceleration can be made using two accelerometers, one at each end of the axle, measuring $\ddot{y}_{rlw}$ and $\ddot{y}_{rrw}$ respectively.

$$\mathbf{z} = \begin{bmatrix} \alpha & \ddot{x} & \ddot{z} & \ddot{y}_{flw} & \ddot{y}_{frw} & \ddot{y}_{rlw} & \ddot{y}_{rrw} & \omega_{flw} & \omega_{frw} & \omega_{rlw} & \omega_{rrw} \end{bmatrix}^T$$

The system is locally controllable when the yaw rate and wheel velocity states are all assigned non-zero process noise variances and the augmented tyre force derivatives are all driven by white noise.

4 A virtual haul truck

To test the tyre force estimator, a comprehensive virtual model of a mining truck, has been developed, see Figure 3. The model has been built using the dynamic modelling package, ADAMS. It is a representation of a 150 tonne mechanical drive truck, with the similar dimensions, masses and suspension and tyre stiffnesses. In order to accurately represent a real haul truck the truck model includes non-linear suspension and tyre characteristics based on the physical measurements given in French (1994). The suspension uses all the moving parts seen on a real truck. Nonlinear stiffness and damping curves are incorporated into the suspension, stiction is included by incorporating dynamic friction into the translational joints of the struts and bumps stops are represented by high increases in stiffness at the limits of strut travel. The tyres are modelled using an advanced tyre model, which incorporates a comprehensive slip analysis to determine tyre forces and moments. The properties of the virtual truck are listed in table 1.

Table 1.Virtual truck model parameters

Parameter	Value
M_t	244500 kg
I_y	1904000 kgm^2
M_{flw}, M_{frw}	2650 kg
M_{axle}	15800 kg
I_{axle}	65250 kgm^2
r_{flw}, r_{frw}	1.453 m
l_f	3.969m
l_r	2.28 m
f_l, f_r	2.2 m
r_l, r_r	2.15 m
a_t	2.15 m
a_s	0.83 m

The Virtual truck is simulated to perform generic truck manoeuvres. During these simulations measurement and input data is exported for use in the EKF. Tyre force data is also recorded from the tyre model to compare with the estimates.

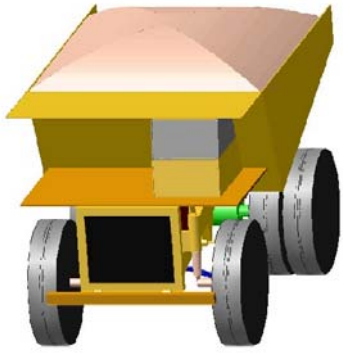

Figure 3: Virtual Haul Truck

5 Simulations

Measurement and input data is exported form the virtual truck at 50 Hz. The measurements are corrupted with noise according to table 2. The EKF is initialised with the truck at rest, with all the initial states set to zero except for the vertical tyre forces which are set at static values. The initial covariance matrix is assigned the identity matrix. The driving noise variances on the tyre force derivatives are typically set to values 2 to 3 times the maximum tyre force rate of change experienced during the manoeuvre. The EKF has been coded in MATLAB.

Table 2. Typical sensor noise variances

Sensor	Noise Variance
Acceleration	0.0025 (m/s^2)^2
Rate	0.0001 (rad/s)^2
Wheel speed	0.0025 (rad/s)^2

Figure 4 plots estimates and the true values of the vertical and lateral tyre forces for a generic coast-down manoeuvre. A coast-down is typically performed to slow a truck as it approaches the dumping area. The virtual truck is initially travelling at 50 km/h, at 40 seconds the drive torque is cut and a 10 degree steering angle is introduced. With the introduction of the steering angle lateral tyre forces are developed. They peak with lateral acceleration and then reduce as the truck slows. During the turn the truck rolls, increasing the vertical forces on the left and decreasing them on the right.

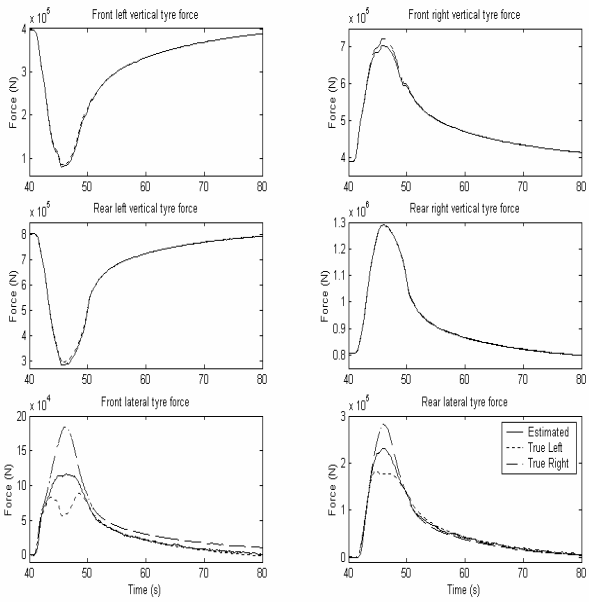

Figure 4. Tyre force estimates during a coast-down

The front and rear vertical tyre force estimates track well during the manoeuvre. However, the consequences of an estimated combined lateral forces is evident in the lateral force plots of Figure 4. As the truck rolls, the reduction in vertical force on the left tyres causes the tyre/road friction threshold to be met. Lateral force is transferred from the left to the right tyre where the higher vertical force enables higher lateral forces. The lateral force estimated will only observe the combined effects of actual left and right lateral forces.

Figure 5 plots the front tyre force estimates for a straight line braking manoeuvre. Here the truck is initially travelling at 50 km/h at 51 seconds braking torques are applied to the front and rear wheels. The braking torques are reacted by longitudinal forces which slow the truck to 3 km/h in approximately 5 seconds. As the truck de-accelerates it pitches forward increasing the front vertical tyre forces and decreasing those at the rear.

The large bias in the front longitudinal tyre force estimates can be mostly contributed to large changes in tyre wheel radius during the braking manoeuvre (there will also be some contribution from neglecting rolling resistance). As the truck brakes it pitches forward, increasing the vertical force and reducing the effective rolling radius of the tyre. If the radius of the wheel reduces the longitudinal tyre force must increase to compensate and keep the balance of the overall torque at the wheel centre. The deficiency in the implemented estimation model is it assumes a constant static tyre radius.

6 Conclusions

This paper shows that it is feasible to estimate the forces that act at the tyre road contact. The required sensor set includes lateral and longitudinal acceleration and yaw rate measured on the truck body. The vertical accelerations and wheel speeds of each wheel. The system inputs include the steering angle, driving and braking torques, suspension strut forces and the force in the rear axle panhard rod. The estimator requires no knowledge of tyre parameters.

Lateral tyre forces cannot be estimated individually, using the proposed model, without additional acceleration or displacement measurements made on the tyres. Assuming it is un-feasible to make these measurements only the combined front and rear lateral forces can be estimated.

In the simulations the force estimates tracked well, however, there was evidence that un-modelled truck dynamics contributed to estimate errors. In further work, a sensitivity analyses is required to quantify the effect of estimation model uncertainties on the force estimates. These uncertainties may include the variance in the rolling radius of tyres, the truck's payload mass and inertias and the position of the centre of mass with respect to sensor position.

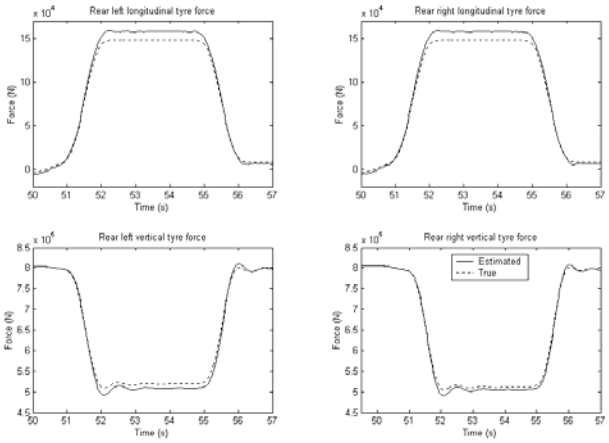

Figure 5. Tyre force estimates during braking

References

1. French, P. (1994). *Investigation of intelligent dumper and hauler suspension system (IDHSS) concept*. ACARP Report C3103.
2. Gelb, A. (1974), *Applied Optimal Estimation*, M.I.T. Press, Cambridge.
3. Martin, J.W, Martin, T.J, Bennett, T.P (1981), *Surface Mining Equipment*, Martin Consultants Inc, Colorado, pp.125-169.
4. Prem H. (1998), *Off-Highway Mine Haul Truck Dynamics Simulation*, SAE Technical Paper Series, 981982.
5. Ray, L.R. (1995), *Nonlinear State and Tire Force Estimation for Advance Vehicle Control*, IEEE Transactions on Control Systems Technology, 3 (1), 117-124.
6. Ray, L.R. (1997), *Nonlinear Tire Force Estimation and Road Friction Identification: Simulation and Experiments*, Automatica, 33 (10), 1819-1833.
7. Reif, K., Gunther, S., Yaz, E., Unbehauen, R. (1999), Stochastic Stability of the Discrete-Time Extended Kalman Filter, IEEE Transactions on Automatic Control, 44 (4), 714-727.